

# Analysis of the Risk of Water Breakout in the Bottom Plate of High-Intensity Mining of Extra-Thick Coal Seams

Shuo Wang<sup>1</sup>, Hongdong Kang<sup>1</sup>, Xinchun Wang<sup>2</sup>

<sup>1</sup>School of Energy Science and Engineering, Henan Polytechnic University, Jiaozuo, China

<sup>2</sup>Technology Institute of Energy Engineering, Shanxi Institute of Science and Technology, Jincheng, China

Email: 446439508@qq.com

**How to cite this paper:** Wang, S., Kang, H. D., & Wang, X. C. (2024). Analysis of the Risk of Water Breakout in the Bottom Plate of High-Intensity Mining of Extra-Thick Coal Seams. *Journal of Geoscience and Environment Protection*, 12, 81-91.

<https://doi.org/10.4236/gep.2024.125006>

**Received:** April 12, 2024

**Accepted:** May 19, 2024

**Published:** May 22, 2024

Copyright © 2024 by author(s) and Scientific Research Publishing Inc.

This work is licensed under the Creative Commons Attribution International License (CC BY 4.0).

<http://creativecommons.org/licenses/by/4.0/>



Open Access

## Abstract

In order to clarify the danger of water breakout in the bottom plate of extra-thick coal seam mining, 2202 working face of a mine in the west is taken as the research object, and it is proposed to use the on-site monitoring means combining borehole peeping and microseismic monitoring, combined with the theoretical analysis to analyze the danger of water breakout in the bottom plate. The results show that: 1) the theoretically calculated maximum damage depth of the bottom plate is 27.5 m, and its layer is located above the Austrian ash aquifer, which has the danger of water breakout; 2) the drill hole peeping at the bottom plate of the working face shows that the depth of the bottom plate fissure development reaches 26 m, and the integrity of the water barrier layer has been damaged, so there is the risk of water breakout; 3) for the microseismic monitoring of the anomalous area, the bottom plate of the return air downstream channel occurs in the field with a one-week lag, which shows that microseismic monitoring events may reflect the water breakout of the underground. This shows that the microseismic monitoring events can reflect the changes of the underground flow field, which can provide a reference basis for the early warning of water breakout. The research results can provide reference for the prediction of sudden water hazard.

## Keywords

Extra-Thick Coal Seam, High-Intensity Mining, Microseismic Monitoring, Water-Surge Hazard, Borehole Peeping

## 1. Introduction

At present, the western mining area is the main battlefield for the development

and supply of coal resources in China (Xie et al., 2019; Yuan, 2018). With the increasing maturity of the integrated mechanized coal mining process, mines with thick coal seams adopt such processes as large mining height, one-time mining, and integrated mining of extra-thick coal seams to recover coal resources (Xu & Wang, 2023; Zhao et al., 2023; Yu et al., 2023). High-intensity mining characterized by large mining height and fast advancing speed causes violent rock movement and obvious mine pressure, and the resulting development of bottom plate fissures can cause further mine water emergence danger, which poses more challenges for water emergence danger prediction and water damage prevention and control (Shi & Lyu, 2023; Guo, 2022; Yin et al., 2021).

In recent years, a large number of scholars have carried out theoretical studies on the danger of bottom plate water breakout, Fan Zhenghong (Fan, 2021) and others used the critical water pressure method to calculate the maximum depth of destruction of the bottom plate of the working face and carried out the prediction of water breakout within the bottom plate fissure; Li Ang (Li et al., 2020) and others put forward the formula for calculating the depth of destruction of the disturbance of the bottom plate with higher accuracy and stronger prediction ability. Dai Gelian (Dai et al., 2023) and others used the weighted rank sum ratio method to evaluate the danger of water breakout in the bottom plate of coal seams. Zhang Chengbin (Zhang & Zhang, 2023) and others used the hierarchical analysis method (AHP) to classify the danger threshold of bottom plate water breakout, and used it to establish the prediction model of coal bed bottom plate water breakout. Qiu Xingguo (Qiu & Li, 2022) established a prediction model of coal mine bottom slab water breakout based on CNN-GCN-BiLSTM, and predicted coal mine bottom slab water breakout through neural network technology. Xiong Xinbiao (Xiong et al., 2023) established a bottom slab water-surge prediction model based on principal component analysis and Logistic regression method, and studied the influence of different variables on water-surge in mines. Wang Songsong (Wang et al., 2023) and others determined the weights of the main control factors of water breakout based on the combination of principal component analysis, coefficient of variation method and CRITIC assignment method, and established the evaluation model of vulnerability index of coal bed floor water breakout to evaluate the risk of water breakout of coal bed floor by zoning. Although the damage depth of the bottom plate and the risk of water breakout can be quickly analyzed through theoretical calculations and mathematical model analysis, which can be used as a reference for the prediction of water breakout in the bottom plate; however, due to the special geological conditions, and the individual variability of the disturbance to the surrounding rock in the process of coal seam mining, there is uncertainty in the theoretical study. Therefore, the theoretical study has uncertainty, in order to accurately obtain the damage pattern of the bottom plate, and it must be combined with the field measurement.

The more widely used and mature means of actual measurement include: borehole peeping method, water-filled leakage amount drilling method, micro-

seismic monitoring method, etc. Zhang Hang (Zhang et al., 2022), Chai Jing (Chai et al., 2022), Dai Chen (Dai, 2019). etc. used the method of borehole peeping to observe the rock layer around the working face, so as to more intuitively respond to the damage of the rock layer. Liu Ruirui (Liu et al., 2022) and others used the water-filled leakage drilling method to measure and analyze the development height of the two zones in the overburden of the working face. Jin Dewu (Jin et al., 2021) and others proposed a method of recognizing water-conducting channels based on the inversion of microseismic energy density and rock fracture connectivity, which was verified in the field by visual resistivity monitoring data. Wang et al., 2022 used a microseismic monitoring system to monitor the activity of the bottom plate coal rock, thus realizing the monitoring of the development of the water-conducting fissure zone.

The existing results of the research are mostly aimed at the mines or workings with low mining intensity in the east-central part of the country, and there are few studies on the danger of water breakout in the bottom plate of high-intensity mining of extra-thick coal seams in the western mining area.

Therefore, this paper adopts the methods of theoretical calculation, microseismic monitoring, and borehole peeping to analyze the danger of water breakout on the bottom plate of 2202 comprehensive workings as the research object. The research results can provide a reference for the analysis of the risk of water breakout in the working face of high-intensity mining of extra-thick coal seams.

## 2. Project Overview

A coal mine in the west is located in the middle and western part of Jungar Coal Field in Ordos City, with a designed annual output of 10 Mt. The average burial depth of the 6# coal seam is 245 m, and the average thickness is 12.37 m. The coal seam has an inclination angle of 08°, with a complex structure, and it is a very thick coal seam that can be mined in the whole area, and the characteristics of the rock properties of the coal seam and the top and bottom slabs are shown in Table 1.

**Table 1.** Lithologic characteristics of coal seam and roof and floor slabs.

Top and bottom plate name	Rock type	Average thickness/m	Petrographic description
basement layer	siltstone	17	Light gray, off-white, thickly laminated, coarse-grained structure, jagged fracture, hard
direct Top	siltstone	8	Light gray, off-white, thickly laminated, fine-grained structure, moderately fissured, hard.
a coal seam	coal	12.1	Coal, stable - more stable seams
direct bottom	shale	4.9	Grayish black, dark gray, thinly laminated, semihard

2202 comprehensive working face is the main mining face of 6# coal seam, the coal thickness in the working face area is 10.74 - 13.50 m, the tendency length is 245 m, the average length of the mineable strike length is 3647 m, and the reserve of the working face is about 12.67 million tons.

The water-bearing layer of the bottom plate of the 6# coal seam is the aureole of 61 m under the bottom plate of the coal seam, and the water influx is 0.032 - 49.72 m<sup>3</sup>/h, and the bottom plate of the water-insulating layer bears to the aureole water pressure of 0.5 - 5.12 MPa, and the water-richness of the local section is stronger, as shown in **Figure 1**, the water-bearing layer of the bottom plate of the 6# coal seam is the aureole tuff, and the water-insulating layer 1 is the rock layer dominated by mudstone and claystone, and belongs to the Benxi Group of the Carboniferous System, and the water-filling channel is the water-conducting fissure zone of the bottom plate of the coal seam.

### 3. Theoretical Calculation of Limit Damage

Limit damage theory (Zhang & Liu, 1990) is the current key theory to study the depth and law of bottom plate disturbance damage. When the coal mining face is mined, the coal wall of the coal mining face as well as the coal pillar on both sides trigger the plastic slip damage of the bottom plate under the supporting pressure.

The slip line mechanics model of mining damage of bottom plate rock body by supporting pressure of coal pillar on one side of comprehensive coal mining face is established to determine the maximum depth and length of the damage zone under the condition of ultimate supporting pressure, and the calculation method and process are as follows:

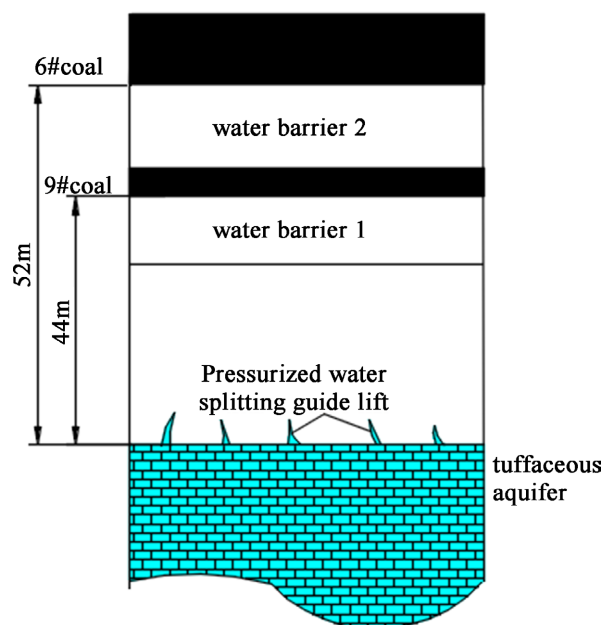


**Figure 1.** Schematic diagram of water-bearing and water-insulating layer in the bottom plate of 6# coal seam.

$$h_1 = \frac{x_0 \cos \phi_1}{2 \cos\left(\frac{\pi}{4} + \frac{\phi_1}{2}\right)} \exp\left[\left(\frac{\pi}{4} + \frac{\phi_1}{2}\right) \tan \phi_1\right] \quad (1)$$

$$D = \frac{x_0 \sin \phi_1}{2 \cos\left(\frac{\pi}{4} + \frac{\phi_1}{2}\right)} \exp\left[\left(\frac{\pi}{4} + \frac{\phi_1}{2}\right) \tan \phi_1\right] \quad (2)$$

$$d = x_0 \tan\left(\frac{\pi}{4} + \frac{\phi_1}{2}\right) \exp\left(\frac{\pi}{2} \tan \phi_1\right) \quad (3)$$

Formula:  $h_1$ —Maximum depth of damage from base plate mining, m;

$D$ —Horizontal distance from the end of the working face to the maximum depth of damage of the rock body of the base plate, m;

$d$ —Maximum length of damage along the horizontal plane of the rock body of the bottom plate in the mining hollow area, m;

$\phi_1$ —Friction angle within the base plate rock,  $\phi_1 = 34^\circ$ ;

$x_0$ —Width of the internal yield zone of the coal body in front of the workings,  $x_0 = 15$  m.

From the above, it can be seen that the factors affecting the damage depth of the coal seam bottom plate mainly include the internal friction angle of the bottom plate rock body and the width of the internal yield zone of the coal body in front of the workings. Under the working condition of integrated mining, the dynamic load impact generated by the top plate pressure will be more intense, and the maximum depth of coal seam bottom plate damage will be generated after the top plate pressure, thus triggering the lagging water breakout.

Calculation can be obtained 2202 working face bottom plate maximum damage depth  $h_1$  is 27.5 m, the maximum damage depth of the bottom plate rock body from the end of the working face horizontal distance  $D$  is 18.54 m, the maximum damage length along the horizontal direction of the bottom plate rock body in the mining hollow area  $d$  is 81.39 m, the bottom plate mining damage sliding line pattern is drawn as shown in **Figure 2**, the bottom plate damage area has been developed to the water barrier layer 1, with a certain water breakout risk. The damage area of the bottom plate has developed to the water barrier layer 1, which has certain risk of water surge.

#### 4. Macroscopic Fissure Peeping of the Base Plate

In order to observe the specific fissure development of the bottom rock layer under the influence of mining in the working face, two downward drilling holes were arranged in the 2202 auxiliary transportation trench. The drill holes were drilled at an angle of  $-20^\circ$ , using 32 mm diameter anti-abruptive drill pipes, with a depth of 40 m. The drill holes were arranged as shown in **Figure 3**. Measuring station I is located at 24 m from the geological drill hole F22, and measuring station II is located at 17 m from the geological drill hole F22, and a drilling peeper is used to observe the fissures of the bottom plate of the working face.

The bottom plate fracture development observed at station I is shown in **Fig-**

**Figure 4.** It can be seen from the analysis of the borehole peep images that radial fissures appeared in the shallow borehole wall in station I, and the borehole wall was deformed and broken with the deepening of the peep. This indicates that the stress is released in the bottom rock layer, which leads to the development of internal cracks in the bottom rock layer and a certain number of cracks in the range of 0 - 26 m from the bottom, and the integrity of the watertight layer is damaged.

The development of fissures in the bottom plate observed at station II is shown in **Figure 5**. It can be analyzed that the radial and lateral fractures are densely distributed in the range of 0 - 10 m from the base plate of the coal seam, and there are a certain number of fractures in the range of 10 - 26 m from the

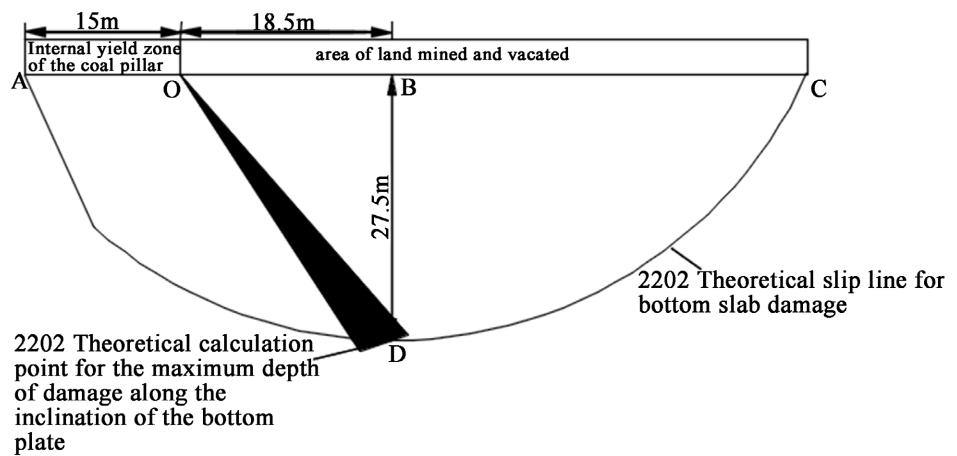


**Figure 2.** Slip line pattern of bottom plate mining failure.

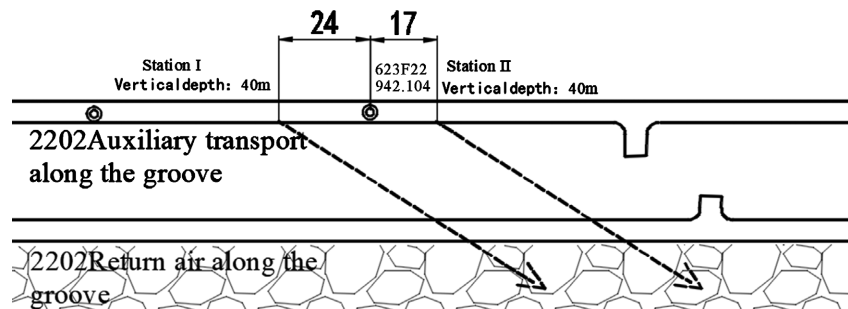


**Figure 3.** Layout of the borehole for observation of cracks in the floor of the working face.

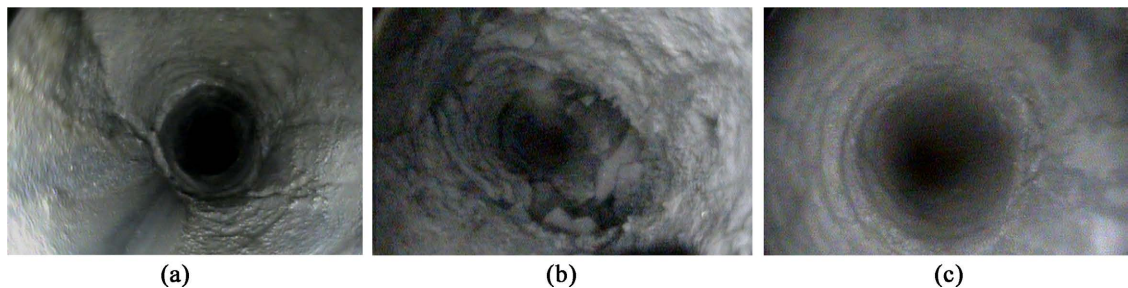


**Figure 4.** Development of cracks in the floor of station I. (a) Depth 1.80 m; (b) Depth 6.80 m; (c) Depth 19.80 m.

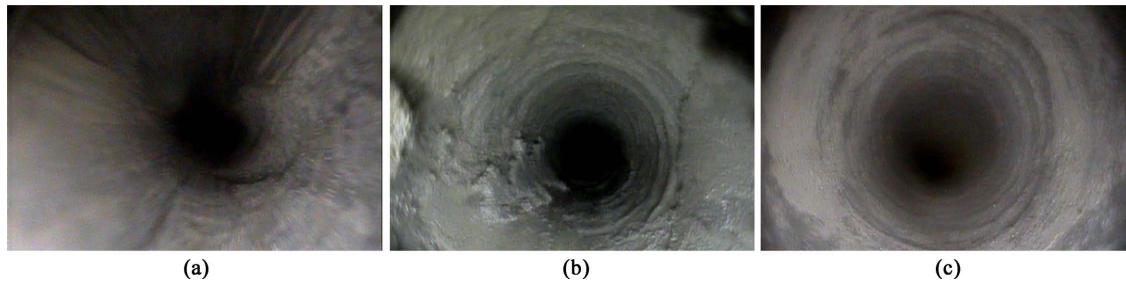


**Figure 5.** Development of cracks in the floor of the station II. (a) Depth 1.50 m; (b) Depth 19.80 m; (c) Depth 26 m.

base plate of the coal seam. After the depth of 26 m from the bottom plate, the hole wall is relatively smooth, and no obvious macroscopic fissures are observed, and with the increase of the depth from the bottom plate, the hole wall is relatively smooth, so it reflects that under the influence of mining in the extra thick coal seam, the bottom plate fissures have been developed up to 26 m, and the fissures have been developed up to the water separation layer 1.

It can be seen from the drill hole peeping image that in the range of 0 - 10 m from the bottom plate of coal seam 6, it is obviously affected by mining, thus generating dense lateral fissures; in the range of 10 - 26 m from the bottom plate, there are a certain number of fissures, and with the deepening of the drilling, it can be seen that the maximum depth of fissure development is 26 m from the bottom plate, the integrity of the watertight layer has been damaged, and there is a risk of water breakout.

## 5. Substrate Microseismic Monitoring

### 5.1. Microseismic Arrangement

Typically, the monitoring sensors are arranged in the underground roadway around the mining area where they are arranged for monitoring. For the geological situation, underground roadway arrangement and mining conditions in this mine, as shown in **Figure 6**, six measurement points are set up in two roadways in the 2202 working face.

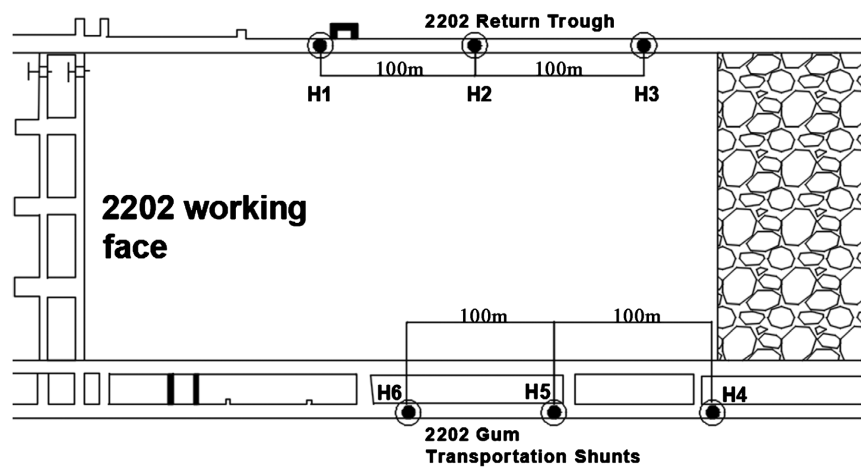


**Figure 6.** Schematic diagram of the layout of the microseismic system.

## 5.2. Microseismic Data Analysis

In the microseismic monitoring of the 2202 working face, a total of 10,100 microseismic events were received, of which 8800 were valid events, with the top plate events accounting for 6400 and the bottom plate events accounting for 2400, and their energies ranged from  $1.0 \times 10^{-1}$  J to  $4.15 \times 10^6$  J, with an average energy of  $7.16 \times 10^3$  J. Based on the spatial location of their occurrences (Z-coordinate) and the relative position of the working face, a statistical map of the plane distribution of microseismic events is plotted in **Figure 7**, the statistical plot of the plane distribution of microseismic events was drawn by Origin mapping software, as shown in **Figure 7**.

During the production process, the energy and number of microseismic events increased significantly and were dominated by small energies, characterized by overall low intensity and stability. According to the statistical map, it can be seen that the depth of influence of 2202 working face mining on the bottom plate is about 26 m, which has been developed to the water separation layer 1, and the collapsed influence range at the edge of the extraction zone is about 60 m. Among them, the microseismic events within the range of 0 - 10 m under the bottom plate are most numerous, which are more intensely influenced by the mining movement, and have the characteristics of the intensive development of the bottom plate destruction zone.

In order to investigate the damage of the bottom plate in the 2202 working face, Origin mapping software was used to map the density distribution of microseismic events along strike and trend (**Figure 8**, **Figure 9**), and it can be seen from **Figure 8** that, in the direction of the strike, the microseismic events mainly occurred in the back-mining area, and most of the microseismic events were centered in the middle of the area. During the monitoring period, microseismic events were relatively evenly distributed in the base plate, mainly developed in the range of 26 m below the base plate (marked by red dotted line in the figure),

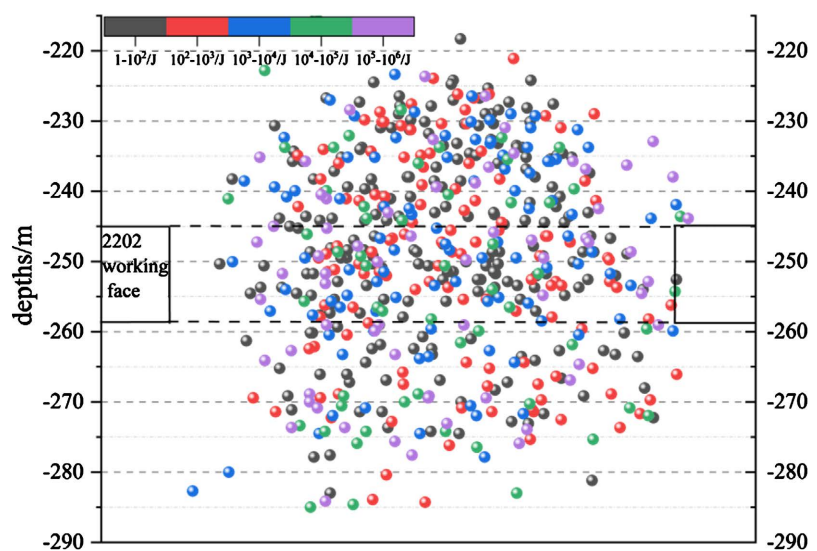


**Figure 7.** Statistical chart of microseismic events.

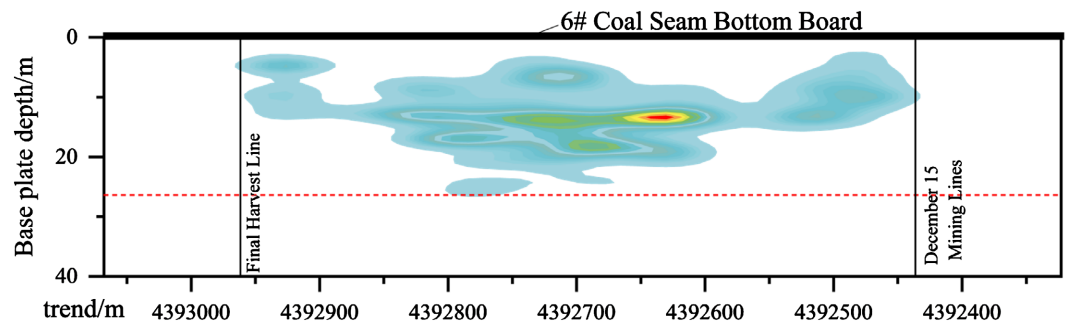


**Figure 8.** Density distribution of microseismic events along strike of floor microseismic events.

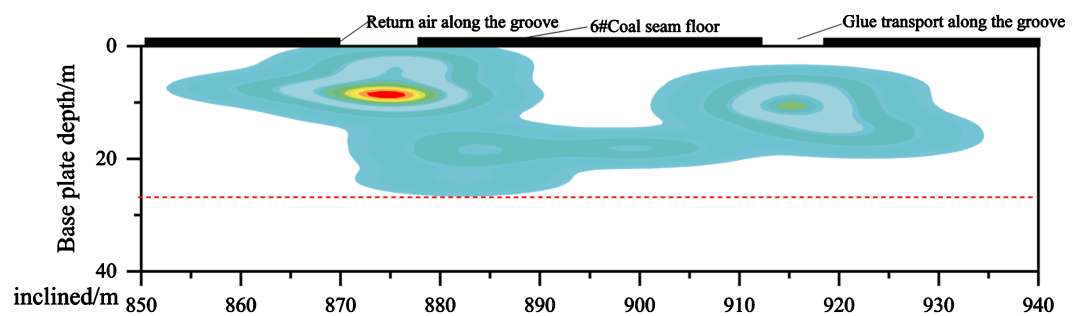


**Figure 9.** Density distribution of microseismic events along the floor along the tendency.

and a small range of concentration appeared in the range of 0 - 10 m below the base plate, which indicated that there was a centralized development of fissures in this range; as shown in **Figure 9**, along the direction of inclination, the microseismic events showed a tendency of first increasing and then decreasing in number, energy, and density; a large number of microseismic events appeared in the return wind trough of the 2202 working face; and a large number of microseismic events occurred in the downwind trough of the 2202 working face. A large number of microseismic events are concentrated along the return air groove of the working face, and extend to the side of the goaf.

### 5.3. Predictive Analysis of Microseismic Sudden Water

Since February 3, a large number of microseismic events have been occurring in the deep part of the return trench when the working face passes through the area of the DF6 fault zone, and the occurring layers are mainly concentrated in the water separation layer 1. microseismic events have increased significantly in the bottom plate of 2202 and the water separation layer 2 since February 10, and microseismic events in the water-bearing layer of the aoar ash have increased and formed a gathering from February 15 to February 17, and the phenomenon of the bottom plate coming out of the return trench was observed in the return trench on February 20, which caused a change in the flow field of the aoar ash water during the mining process in this area. During the mining process in this area, the fault zone caused changes in the flow field of the ash water. The high-pressure aureole water caused karst collapse and vacuum suction erosion, which led to the generation and aggregation of microseismic events.

Under the same flow field, before the water emergence in the back-mining trench, the microseismic monitoring area has already monitored the abnormal behavior, and the microseismic events appear to increase and gather phenomenon, which fully demonstrates that the microseismic monitoring system has a certain prediction ability of water breakout.

At present, 2202 working face has completed safe mining. The site has modified its bottom plate by grouting the rock layer of the bottom plate, successfully passed through the area of DF6 fault zone, ensured the integrity of the water-isolating layer of the bottom plate, and weakened the influence of the water damage of the Austrian ash, so as to ensure the safe mining of the 6# coal seam.

## 6. Reaching a Verdict

1) According to the theory of limit damage, the maximum depth and length of the damage area of 2202 working face are analyzed, and the maximum depth  $h_1$  and length  $D$  of the damage area are 27.5 m and 81.39 m respectively, and the damage area of the bottom plate has been developed to the water-trap layer 1, which is at a certain risk of water breakout.

2) Borehole peeping at the bottom plate of 2202 working face shows that the depth of bottom plate fissure development reaches 26 m, and the integrity of water barrier layer is damaged, and there is a risk of water breakout; after anomalous area appears in microseismic monitoring, the bottom plate out of the downwind trench occurs in the field with a lag of one week, which shows that the microseismic monitoring event can reflect the changes of underground flow field, and it can provide a reference for the early warning of water breakout. This research result can provide reference for the prediction of sudden water hazard.

3) The bottom plate of 2202 working face has been safely mined back after the field engineering test of grouting modification. This research can provide a mature program for the prevention and control of water breakout in the bottom plate of high-intensity mining of extra-thick coal seams.

## Conflicts of Interest

The authors declare no conflicts of interest regarding the publication of this paper.

## References

- Chai, J., Qiao, Y., Gao, S. G. et al. (2022). Roof Stability Evaluation of Large Section Open-Off Cut in Lower Slice of Slicing Mining. *Journal of Mine Automation*, 48, 21-31.
- Dai, C. (2019). Research on Deformation and Failure Characteristics of Narrow Coal Pillar Mining Roadway in Hengsheng Coal Mine and the Support Optimization Technology. *Coal Engineering*, 51, 70-73.
- Dai, G. L., Wu, P. N., Niu, C. et al. (2023). Weighted Rank Sum Ratio Method Was Applied to Evaluate Water Inrush Risk of Floor. *Coal Technology*, 42, 109-113.
- Fan, Z. H. (2021). Prediction of Water Inrush from Floor of Working Face. *Coal Tech-*

- nology*, 40, 142-144.
- Guo, G. Q. (2022). Floor Failure Law of Extra-Thick Coal Seam in Fully Mechanized Caving Mining. *Coal Geology & Exploration*, 50, 107-115.
- Jin, D. W., Liu, J., Xu, F. et al. (2021). Method of Determining of Pre-Drainage Standard in Water-Decrease Mining of Shallow Seam in Yushen Mining Area. *Journal of China Coal Society*, 46, 220-229
- Li, A., Mou, Q., Liu, C. Y. et al. (2020). Study on the Damage Depth of Bottom Plate Disturbance under the Influence of Multiple Factors in the North Wei Coal Field. *Coal Engineering*, 52, 138-143.
- Liu, R. R., Liu, Y., Fang, G. et al. (2022). Law of Overburden Failure and Roof Water Damage in Yuandatan. *Coal Mine Safety in Coal Mines*, 53, 82-91.
- Qiu, X. G., & Li, N. (2022). Prediction Model of Water Inrush from Coal Floor Based on CNNGCN-BiLST. *Coal Technology*, 41, 84-87.
- Shi, X. C., & Lyu, G. L. (2023). Risk Assessment of Water Inrush from over Burden High-Level Bed Separation in Extra-Thick Coal Seam Mining. *Safety and Environmental Engineering*, 30, 109-117.
- Wang, J., Li, B. F., Jiang, Q. P. et al. (2022). Identification of Damage Depth Caused by Long-Wall Mining Using Microseismic Technique. *Journal of Mining and Strata Control Engineering*, 4, Article ID: 053512.
- Wang, S. S., Dai, G. L., & Niu, C. (2023). Study on Water Inrush Risk of Coal Seam Floor Based on Combination Weighting Method. *China Energy and Environmental Protection*, 45, 98-104+110.
- Xie, H. P., Wu, L. X., & Zheng, D. Z. (2019). Prediction on the Energy Consumption and Coal Demand of China in 2025. *Journal of China Coal Society*, 44, 1949-1960.
- Xiong, X. B., Xie, X. G., Yang, P. J. et al. (2023). Research on Water Inrush Risk of Mine Floor Based on PCA-Logistic Regression Model. *Safety in Coal Mines*, 54, 176-181.
- Xu, Y. Y., & Wang, L. (2023). Prevention and Control Technology and Application of Hidden Danger of Coal Spontaneous Combustion in Top Slicing Fully Mechanized Caving Working Face in Thick Coal Seam. *Coal Technology*, 42, 160-164.
- Yin, S. X., Lian, H. C., Xu, B. et al. (2021). Deep Strip Mining: Heritage and Innovation. *Coalfield Geology and Exploration*, 49, 170-181.
- Yu, B., Kuang, T. J., Yang, J. X. et al. (2023). Analysis of Overburden Structure and Evolution Characteristics of Hard Roof Mining in Extremely Thick Coal Seam. *Coal Science and Technology*, 51, 95-104.
- Yuan, L. (2018). Strategies of High Efficiency Recovery and Energy Saving for Coal Resources in China. *Journal of China University of Mining & Technology (Social Sciences)*, No. 1, 3-12.
- Zhang, C. B., & Zhang, P. (2023). Mine Floor Water Inrush Prediction Model and Application Based on AHP Vulnerable Index Method. *Safety in Coal Mines*, 54, 172-179.
- Zhang, H., Yang, Y. K., & Wang, C. L. (2022). Research on Mining Technology of Interlaced Distribution of Coal Seam Group Pedal Empty Three Coal Seam. *Coal Technology*, 41, 53-57.
- Zhang, J. C., & Liu, T. Q. (1990). On the Depth and Distribution Characteristics of Mining Fissure Zones in Coal Seams. *Journal of China Coal Society*, No. 2, 46-55.
- Zhao, B., Wang, Y. et al. (2023). Mechanism and Prevention and Control Technology of Mine Earthquake in Fully Mechanized Top Coal Caving Face in Extra Thick Seam: Taking Longwanggou Coal Mine as an Example. *Science Technology and Engineering*, 23, 12451-12457.